LPI Waveform Design Using Chirplet Graphs

Bijan G. Mobasseri
Electrical & Computer Engineering
Villanova University
Villanova, PA,19085
bijan.mobasseri@villanova.edu

Amro Lulu
Electrical & Computer Engineering
Villanova University
Villanova, PA,19085
alulu01@villanova.edu

***Abstract*—The Low Probability of Intercept (LPI) signals are of great interest in underwater acoustics. LPI signals are designed such that their presence is difficult to detect, hence taking countermeasures against them are less likely. The traditional method of LPI waveform design is to spread the signal energy in time and/or frequency thus making it indistinguishable from ambient noise. In this paper, we propose a method of energy dispersal that is based on the formalism of chirplet graphs. The parameters of the chirplet graph constitute the "secret key" for the detection of the signal. Detection is accomplished by accumulating the outputs of a filter bank along the same path used by the source. The idea is that although the signal to noise ratio for any one chirplet may not be enough for reliable detection, their sum along the path used by the source will reach the threshold of detectability based on a required false alarm rate. This accumulated local correlations is then tested in a likelihood ratio test. Unauthorized detectors will most likely follow a wrong path and their accumulated energy will fail detection. We show the strength and limitations of the proposed LPI waveform at various ranges using a simulated underwater acoustic channel.**

I. Introduction

One of the most desirable properties in underwater acoustics is stealth. The challenge is to observe the target without being noticed[1]. Other applications may involve maintaining a quiet posture for reasons related to marine life or keeping a low profile in an underwater acoustic network. What is common to all LPI waveforms is energy dispersion. By spreading the energy over a wide time and frequency plane, the signal can become indistinguishable from the ambient noise. Spread spectrum is the classical method whereby the energy of the signal is spread over a bandwidth much larger than baseband using various spreading codes such PN-sequences or Barker codes. In this work we propose a new LPI waveform design framework using the formalism of the chirplet graphs[2].

Chirps, specifically linear chirps (LFM), are the waveforms of choice in sonar. They decouple range resolution and pulse length without sacrificing power. The problem is, other than controlling the power, LFM waveforms do not have an inherent LPI capability.This weakness can be addressed by replacing a single long pulse with a sequence of shorter LFMs, or chirplets, each identified with specific offset and slope drawn from a codebook which is only available to the intended receivers. Individual chirplets remain well below ambient noise level and are only detectable when their energies are combined by traversing a predetermined path through the graph. Detection of a single chirplet, even with known offset and slope, should not be possible by the target. The only statistically reliable detection of the LPI signal is possible if the local correlations are summed along the correct path in the graph known only to authorized detectors.

II. LPI Concept and Chirplet Graph

The LPI concept arises from a desire to make sonar broadcasts appear indistinguishable from the ocean ambient noise noise while being detectable at the intended receivers. The best known application is perhaps target surveillance, but there are others. In the following we define a framework for LPI as well as the strengths and weaknesses that receiving platforms might have in detecting the signal. We then present a new waveform design methodology for the LPI signals.

A. LPI Framework

There are a variety of applications where it is desired to conceal the presence of signals in the ocean environment. The best known application is target surveillance and tracking. The idea here is to illuminate the target covertly by ensuring that the probe signal remains below the detection threshold at the target. A target that is being probed by an LPI signal is not aware of the presence of the surveillance platform and is unlikely to alter its course or mission because of it. Often, LPI is cast as a means to covertly observe a target. However, this is not the only application area. LPI is also applicable to underwater communication between sea vessels or among the nodes of a sensor network. The idea is to keep source levels low for interference reduction or to conceal the presence of an underwater communication network. There are other situations where a quiet posture is desirable. Examples include regulatory constraints for the protection of marine life and other environmental concerns.

In the context of target tracking, we define the *source* as the platform where the sonar probe originates and the

978-0-933957-43-5 ©2015 MTS

target as the object of surveillance. It has been stated that the source is at a fundamental disadvantage relative to the target because of the two-way path loss[1]. However, there are also disadvantages that are unique to the target. For example, the target cannot employ an optimum detector because it has little to no prior knowledge of the waveform it is trying to detect. A robust detector for such a scenario is no better than a simple energy detector, or radiometer. The energy detector continuously measures the ambient energy and compares it to a threshold. Any rise above the threshold indicates the presence of an LPI signal. Energy detectors have been extensively studied in cognitive radio and spectrum sensing literature[3]. In fact, it could be argued that LPI and cognitive radio share some conceptual similarities in that they both try to establish the minimum required SNR for the detection of extremely weak signals in noise[4]. The target suffers from another disadvantage that the source does not. The energy detector working with imprecise knowledge of noise power faces the so-called "SNR wall"[5]. SNR-wall is a phenomenon that arises from an imprecise knowledge of ambient noise power. It is the SNR below which an energy detector fails to to detect a signal regardless of the length of observation time. For typical uncertainties in noise power measurement, the SNR wall is -6 dB[6]. This is a fairly high SNR in underwater acoustic channels. In contrast to the target, the source is aware of the waveform structure and can implement a matched filter, which does not suffer from the shortcomings of the energy detector. For a given probability of false alarm and probability of detection, the matched filter enjoys a favorable SNR margin over the energy detector under equivalent conditions.

B. The Chirplet Graph

An effective LPI signal that succeeds in evading detection must be indistinguishable from ocean ambient noise at the target. This goal is often achieved by using low power signals of long duration. By increasing the observation interval, the source is able to overcome the ambient noise whereas the target encounters the SNR wall. LFM pulses have long been a favorite but they do not inherently have an LPI capability. In this work, we replace the single LFM pulse with a sequence of chirplets whose interconnections are described by a chirplet graph[2].

Chirplets are a family of multiscale, windowed chirps defined over intervals $I_k = [(k-1)2^{-i}, k2^{-i}]$ where $k = 1, 2, \dots, 2^i$. For example, assuming unit time interval, at scale $i = 3$ the chirplets are defined over 8 equal length segments, $I = [\{0, 1/8\}, \{1/8, 1/4\}, \dots, \{7/8, 1\}]$. A chirplet graph "codebook", specifies a family of functions defined over a discrete set of allowable slopes and offsets $\{\alpha_k, \beta_k\} \in \mathcal{M}$. A subset of $\mathcal{M}$ is used as the key that defines the chirplet graph. This key is needed by the receiver to traverse the graph in the same order

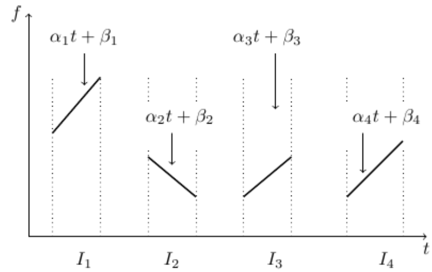

Fig. 1. Rendition of a chirplet graph. Each chirplet is characterized by its own offset and slope.

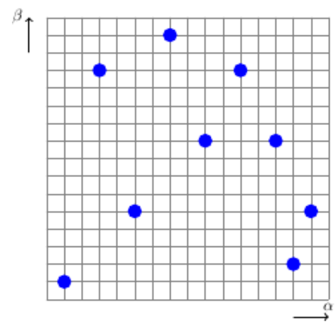

Fig. 2. The (α, β) map specifying the LPI waveform. Dots represent the slope and offset of the individual chirplets.

used by the source.

$$f_{I_k}(t) = A_k e^{j2\pi(\beta_k t + \frac{1}{2}\alpha_k t^2)} \mathbf{1}_{I_k}(t), 0 \le t \le T \quad (1)$$
$$\mathbf{1}_{I_k}(t) = 1, t \in I_k$$

From a collection of chirplets, a longer pulse is produced by sequencing the chirplets in a particular order specified by the slope/offset dictionary. An N segment LPI signal consisting of N chirplets is defined below.

$$x(t) = \sum_{k=1}^{N} f_{I_k}(t) \mathbf{1}_{I_k}(t), 0 \le t \le T \quad (2)$$

A graphical representation of (2) is shown in Fig. 1. As a graph, the chirplets are identified by the set (V, E) where V are the vertices and E are edges. The vertices are pairs of all permissible slopes and offsets. Edges define the adjacency relationships between the chirplets. In the context of LPI, the adjacency is intentionally random. Chirplet graphs were originally proposed for the detection of chirps with unknown structure in noise. The detection of the underlying chirp is accomplished by local correlations along a path in the chirplet graph that produces the highest match score. It is a template matching approach.

The concept using the chirplet graph as an LPI framework is as follows. A single chirp with known offset and slope is replaced with multiple low energy chirplets, each with a different offset and slopes. The offsets and slopes

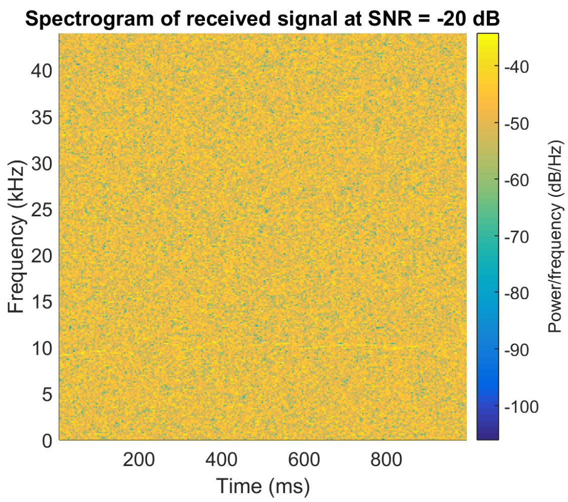

Fig. 3. Spectrogram of the LPI signal at 4500m and SNR=-20dB. This is the edge of visibility.

are drawn from a codebook known only to the source. To meet the basic requirement of and LPI waveform, the chirplet graph must have the following properties. First, chirplets as a whole must remain undetectable by the energy detector at the target at some specified range/SNR. Second, the same chirplet graph must be detectable at a lower SNR by the source to allow for the two way path loss. Third, individual chirplet must be undetectable at the target even if match filtered with known parameters. Fourth, the chirplet graph must only be detectable by accumulating the individual chirplet energies along the same path used by the source. This path is captured in a key and should only be available to the source or other authorized detectors.

III. LPI Detection In The Chirplet Graph

Let $\mathbf{x} = \{x(t), t = 0, \ldots, (M-1)T_s\}$, and $\mathbf{y} = \{y(t), t = 0, \ldots, (M-1)T_s\}$ be the transmitted and received signals, respectively with M the number of samples in the record and T_s the sampling interval. The acoustic channel is characterized by the complex gain factor $\mathbf{h}$ that models random fluctuations in amplitude and phase of the received signal. Depending on the coherence time of the channel and signal duration T, $\mathbf{h}$ may be treated as quasi-stationary during the observation interval. Note that the observation interval is much shorter for the source as it detects each chirplet separately. Following the conventional notation for the null and alternate hypothesis H_0 and H_1, the received signal is given by

$$\begin{cases} \mathcal{H}_0: & \mathbf{y} = \mathbf{n} \\ \mathcal{H}_1: & \mathbf{y} = \mathbf{h}\mathbf{x} + \mathbf{n} \end{cases} \tag{3}$$

Where noise $\mathbf{n} \sim N(0, \sigma_n^2)$. In the following, we explore the scenarios that play out, both at the target and at the source.

A. At Target

Without prior knowledge of the waveform, the target necessarily uses a blind energy detector and computes the following test statistic.

$$T(\mathbf{y}) = \frac{1}{M}\sum_{m=1}^{M}|\mathbf{y}(m)|^2 \underset{H_0}{\overset{H_1}{\gtrless}} \gamma \tag{4}$$

It is well known that for large M the distribution of $T(\mathbf{y})$ is Normal under both hypothesis and the probabilities of false alarm(P_{fa}) and detection (P_d) are governed by the Q-function[7]. It is well known that if the observation interval available to the target is long enough the signal will be eventually detected. However, the target is constrained by the SNR wall that cannot be overcome by the length of the sensing interval. Operating blind, the target can at best try to detect a rise in the background energy level compared to the ambient noise. It cannot take advantage of the structure of the chirplet graph, however. Moreover, chirplets are designed in such a way to individually remain undetectable even if the target has somehow obtained the parameters of a single chirp and attempts to detect it by a matched filter. We will explore the ranges and SNRs that this attempt can or cannot be successful.

B. At Source

Detection of the chirplet graph is based on the accumulation of local correlations of the received signal with the library of chirplets used at the source. While the individual local correlations may not be reach statistical significance, their sum along the path used by the source will.

The received signal vector is segmented into N blocks with $p = M/N$ samples in each segment. The data in the kth segment is denoted by $\mathbf{y}_k = \{y(t), t = kp, kp+1, \ldots, (k+1)p-1)\}$ with $k = 0, 1, \ldots, (N-1)$. Similarly, the kth chirplet vector is defined by $\mathbf{f}_{I_k} = \{f_{I_k}(t), t = kp, kp+1, \ldots, (k+1)p\}$. In each segment I_k, a Z-score is computed by sampling the output of the filter matched to f_{I_k}

$$\begin{aligned} r_k &= <\mathbf{y}_k, \mathbf{f}_{I_k}>, k = 1, \ldots, N \\ \mathbf{r} &= (r_1, r_2, \ldots, r_N) \end{aligned} \tag{5}$$

Where $< . >$ is the inner product operator. When the kth segment is match filtered with the corresponding $\mathbf{f}_{I_k}$, the response under $\mathcal{H}_0$ and $\mathcal{H}_1$ are

$$r_k|\mathcal{H}_1 = \mathbf{h}||\mathbf{f}_{I_k}||^2 + <\mathbf{n}, \mathbf{f}_{I_k}> \tag{6}$$

$$r_k|\mathcal{H}_0 = <\mathbf{n}, \mathbf{f}_{I_k}> \tag{7}$$

The decision rule is based on accumulating r_k over the length of the chirplet graph and thresholding it.

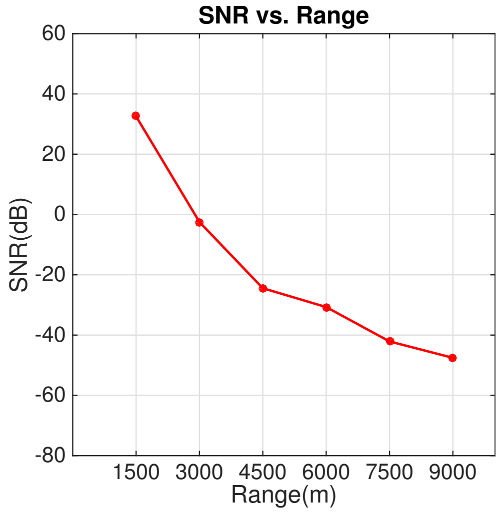

Fig. 4. SNR vs. Range plot for the channel in Table 1

$$T(\mathbf{r}) = \frac{1}{N}\sum_{k=1}^{N}|r_k| \underset{H_0}{\overset{H_1}{\gtrless}} \gamma \tag{8}$$

The distributions of $|r_k|$ under $\mathcal{H}_0$ and $\mathcal{H}_1$ are Rayleigh and Rice, respectively. The distribution of $T(\mathbf{r})$ is found empirically and thresholded to detect the LPI signal. The result is a series of ROC curves that collectively describe the performance of the proposed LPI signal. For large N, the distribution can be approximated as Normal per the Central Limit Theorem. However, in general, there is no exact closed form expression for the distribution of the sum of Rayleigh random variables[8]. The false alarm and miss probabilities are found as follows.

$$\begin{aligned} P_{fa} &= P(T(\mathbf{r}) > \gamma|H_1) \\ P_m &= P(T(\mathbf{r}) \leq \gamma|H_0) \end{aligned} \tag{9}$$

The equivalent ROC curves can be used as design references to establish the boundaries of detectability at both the target and the source.

IV. Simulation Results

The detection of the proposed LPI signal is evaluated in a simulated acoustic channel described in Table 1. The first simulation result shows the variation of the SNR vs. range, Fig. 4. For the given source level, the SNR ranges from a high of 35 dB at 1500m to -42 dB at 9000m. Interestingly, the downward slope of the curve moderates at farther distances.

A. At Target

The target can do no better than an energy detector. The energy detector integrates over a time period that it suspects to be the length of the LPI pulse and then thresholds the response. Setting the threshold is not an easy problem for the target. That is why the chirplets must be designed in such away as to make sure the response of the energy detector stays below the target's threshold. The first requirement of any LPI signal is that it be "undetectable" at the target. However, the notion of undetectability is not well defined in the literature. We define undetectability as operating on the "chance line" of the ROC curves. This is the 50/50 line where the target is under highest uncertainty. This situation arises when the histogram of the noise completely overlaps that of the test statistic with signal present. In effect, the signal is indistinguishable from ambient ocean noise. The SNR corresponding to the chance line is a key design reference. In the absence of any prior information about the waveform, the energy detector is the best option for the target. The corresponding ROC curves are shown in Fig. 5 with the chance line occurring at SNR=-30 dB. At the given source level and the channel described in Table 1, this SNR is reached at about 6000m from the source. Therefore, -30 dB is the target's SNR wall; a threshold below which the LPI signal is indistinguishable from ambient noise. Although the target might experience a wall much sooner, say -6 dB, depending on its knowledge of ambient noise power. Operating on the chance line may be too stringent a requirement, however. Even at SNR=-25 dB, the energy detector is still performing very poorly. This allows the target to be about 1500m closer and still fail to detect the LPI signal.

TABLE I
Simulated Acoustic Channel

Parameter	Value
Source	Chirplet chain, 1sec, 9500 Hz-10500 Hz
Source level	210 dB re $1\mu Pa$
Ocean depth	200m
Source/receiver depth	50m
Range	1500m-9000m
No. of multipath	Variable
Surface/bottom bounce	Variable
Ambient noise	Sea State 2 (Wenz curves)
Volume attenuation	Thorp Attenuation
Wind speed	10 mph
Surface model	McDaniel Surface
Bottom model	Jackson Bottom
Ocean bottom	Medium sand
Sound speed profile	Constant 1500m/sec.
Eigenrays	Variable
Max. surface/bottom bounces	Variable

B. At Source

The source receiver is a bank of matched filters tuned to each chirplet in the chirplet graph. The goal is to make

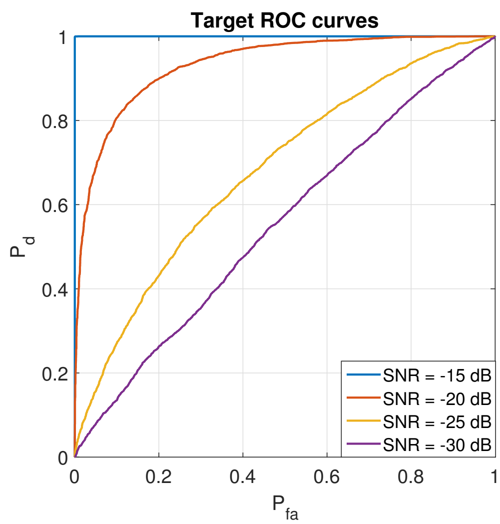

Fig. 5. Energy detector ROC curves at the target. At SNR=-30 dB the signal is indistinguishable from ocean ambient noise.

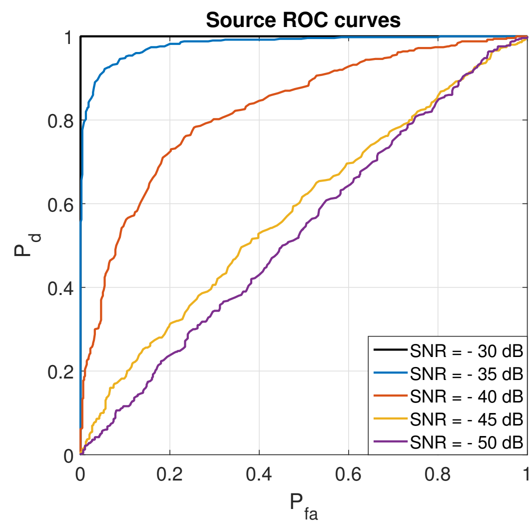

Fig. 7. The ROC curves at the source. Detectability defined by the chance line is SNR=-50 dB, 20 dB below the energy detector.

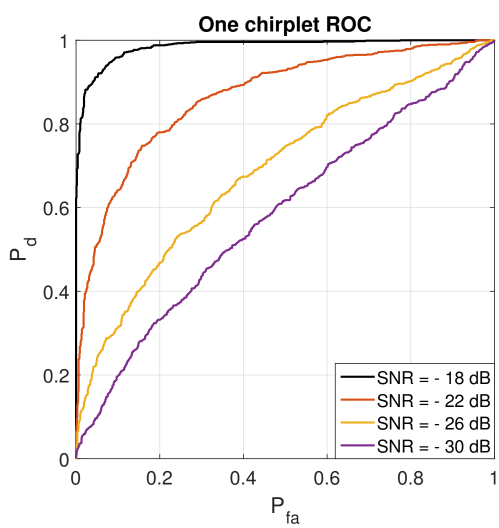

Fig. 6. The ROC curves show the SNR at which a single chirplet remains undetectable by the target even if match filtered. SNR=-30 dB is consistent with the SNR wall of the target's energy detector.

the knowledge of any single chirplet insufficient for the detection even if the target has somehow obtained the key. This requirement is tested in Fig. 6 using a 100-chirplet graph. It is assumed that the target somehow knows, or has found out, the slope and offset frequencies of a single chirplet or is trying to sweep over the spectrum to find the right match. Fig. 6 shows that at SNR=-30 dB, where the entire pulse was undetectable by the energy detector anyway, the target also fails to detect a single chirplet even if it knows what to look for. Even at SNR= -22 dB, and a P_{fa}=0.05, the P_d is only 50%. However, at that SNR it has better luck detecting the entire pulse using the blind energy detector.

Fig. 7 shows what the source can do with the full knowledge of the chirplet graph. Above 90% P_d is achievable at 10% P_{fa} at SNR=-35 dB. Considering that the SNR at the target should be -25 dB or higher, this leaves the source with about a 10 dB margin. For example, the SNR=-25 dB corresponds to roughly 4500m range. The source can tolerate an additional 10 dB loss in SNR. At this range, 10 dB SNR loss corresponds to about an additional 2500m. Although this is not enough for the echo to return to the source, it is still a valuable margin in multistatic sonar allowing hydrophones to be up to 7000m away from the source. Also, the chance line for the the chirplet graph detector is at SNR=-50 dB, 20 dB lower than that of the energy detector. In other words, it takes an additional 20 dB loss for the two detectors to perform equally.

C. *Graph Length*

It is possible to design a chirplet graph of any length. Longer graphs covering the same time span have more chirplets but each has a smaller energy. This helps the objective of making the individual chirplets undetectable even if the target has somehow obtained the chirplet key. Fig. 8 and Fig. 9 are plots of P_d vs. SNR at 5% false alarm rate. They show the trade-off between the short and long chirplet graphs. In Fig. 8, the curves for detecting a single known chirplet and the blind energy detector are nearly coincident. This shows that a single chirplet, even if it is known, is undetectable by the target. The matched filter does no better. Fixing the P_d at 80%, the source needs SNR=-32 dB while both the energy detector and the single chirp detector need at least -20 dB. The 12 dB margin translates to additional range advantage for the source. For example, the target can be as close as 4000m from the source (the range at which SNR=-20 dB) and still fail to detect the LPI

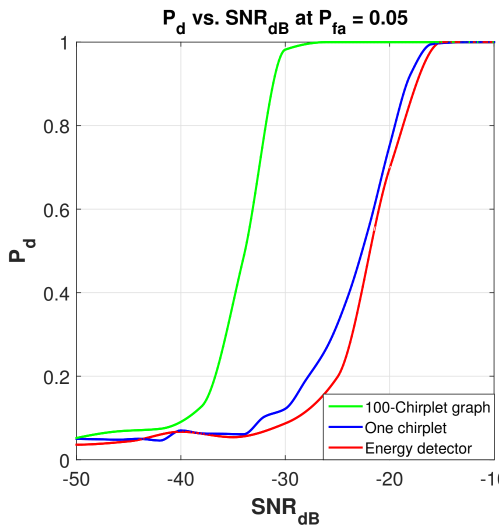

Fig. 8. Using a large number of low energy chirplets reduces the chance of detecting a single chirplet. The matched filter works no better than the energy detector.

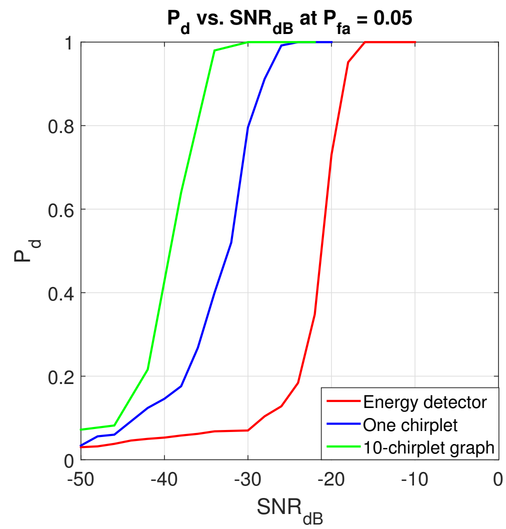

Fig. 9. Choosing few but long chirplets extends the range of covert detectability for the source, but increases the probability of detecting a single chirplet of known form.

signal but the source can detect the chirplet graph at an effective range of 6000m (where SNR=-30 dB) for a 2000m additional range.

For the 10-chirplet graph in Fig. 9, the energy detector performs the same as before but the SNR required by the source with full access to the graph is reduced to -36 dB. This is a 4 dB advantage over the 100-chirplet graph. The downside is that a single chirplet can be detected with $P_d = 0.8$ at SNR=-30 dB. This is about 10 dB lower than the 100-chirplet graph, assuming the target has somehow obtained the key for one chirplet. If this possibility is remote, then a 10-chirplet graph outperforms the longer graph. Another point is that the security of the key is greatly enhanced by the 100-chirplet graph. Having to search a larger key space is an advantage. In addition, since matched filtering of a single chirplet performs no better than the blind energy detector, it would be difficult for the target to get a hook on the chirplet graph and begin to replicate the detection at the source.

V. Conclusions

In this work we have reported on the development of a new framework for the design of LPI signals. The idea is to replace a single LFM chirp with a chain of low energy chirplets, each with a slope and offset frequency known only to authorized detectors. This set is the detection key. The individual chirplets are made to lie below target's SNR wall and can only be detected as a whole when local energy is accumulated along the path in the graph known only to the intended detectors. We showed that the blind energy detector is at a 12 to 16 dB disadvantage relative to the source, translating to additional 4000m in range for the source.

References

[1] P. Willett, J. Reinert, and R. Lynch, "LPI waveforms for active sonar?," in *Aerospace Conference, 2004. Proceedings. 2004 IEEE*, March 2004, vol. 4, pp. 2236–2248.

[2] E. J. Candes, P. R. Charlton and H. Helgason, "Detecting highly oscillatory signals by chirplet path pursuit," *Applied and Computational Harmonic Analysis*, vol. 24, pp. 14–40, 2008.

[3] A. Mariani, A. Giorgetti, and M. Chiani, "Energy detector design for cognitive radio applications," in *International Conference on Waveform Diversity and Design*, Aug 2010, pp. 53–57.

[4] R. Tandra, S. M. Mishra, and A. Sahai, "What is a spectrum hole and what does it take to recognize one?," *Proceedings of the IEEE*, vol. 97, no. 5, pp. 824–848, May 2009.

[5] R. Tandra and A. Sahai, "SNR walls for signal detection," *IEEE J. Sel. Topics Signal Process.*, vol. 2, no. 1, pp. 4–17, February 2008.

[6] Oude Alink, M.S. and Kokkeler, A.B.J. and Klumperink, E.A.M. and Smit, G.J.M. and Nauta, B., "Lowering the SNR Wall for Energy Detection Using Cross-Correlation," *IEEE Trans. Veh. Technol.*, vol. 60, no. 8, pp. 3748–3757, 2011.

[7] G. Yu, C. Long, M. Xiang and W. Xi, "A novel energy detection scheme based on dynamic threshold in cognitive radio systems," *Journal of Computational Information Systems*, vol. 8, no. 6, pp. 2245–2252, March 2012.

[8] J. Hu and N.C. Beaulieu, "Accurate simple closed-form approximations to rayleigh sum distributions and densities," *Communications Letters, IEEE*, vol. 9, no. 2, pp. 109–111, Feb 2005.